

# Coherent control of light pulse propagation in a Raman induced grating

V.G. Arkhipkin<sup>1,2\*</sup> and S.A. Myslivets<sup>1,3</sup>

<sup>1</sup>*Kirensky Institute of Physics, Federal Research Center KSC SB RAS,  
50, Akademgorodok, Krasnoyarsk 660036, Russia*

<sup>2</sup>*Laboratory for Nonlinear Optics and Spectroscopy,  
Siberian Federal University, Krasnoyarsk 660079, Russia and*

<sup>3</sup>*Department of Photonics and Laser Technology,  
Siberian Federal University, Krasnoyarsk 660079, Russia*

We study light pulse propagation in a dynamically controllable periodic structure (grating) resulting from Raman interaction of a weak probe pulse with a standing-wave pump and a second control laser field in the N-type four-level atomic media. The grating is induced due to periodic spatial modulation of the Raman gain in a standing pump field (Raman gain grating). We show that it is possible to control both the probe pulse amplitude and the group velocity of the pulse from subluminal to superluminal by varying the pump or control field. Such a grating is of interest for the all-optical switch and transistor.

PACS numbers: 42.50.Gy, 42.65.Dr

## I. INTRODUCTION

Propagation of light in periodic structures has been an attractive field of research in recent years. Photonic crystals (PCs) represent a broad and special class of structures with the periodicity of the refractive index (the real part of the dielectric constant) on the wavelength scale in one, two, or three dimensions [1]. They have optical band gaps, which offers a possibility to control the propagation of light in a way similar to the control of electron flow in semiconductors. Additional functionality can be created by including absorbing or amplifying features into the structure thus producing PCs with complex dielectric indices [2]. The great opportunities for creating reconfigurable PC offer the optically-induced gratings [3]. In particular, such structures could be created by using electromagnetically induced transparency (EIT) [4] when the strong-coupling laser field is replaced by a standing wave [5, 6]. A standing wave driving configuration has been proposed to induce spatially periodic quantum coherence for generation of PBG [6–8] and dynamic generation of stationary light pulses [9, 10]. These structures are also referred to as an electromagnetically induced absorption grating (EIAG) [11]. EIAG may be utilized for diffracting [12], switching [11] and compressing [13] the probe field. This scheme is also used for atoms localizing in a standing-wave field [14, 15].

An alternative approach is based on using the Raman gain effect [16] in three- and four-level media where we can control amplification of the probe (signal) field. It has been shown that slow [17] and fast [18] light as well as a gain-assisted giant Kerr effect [19] can be obtained by using Raman gain medium. A fast Kerr phase gate using the Raman gain method has been experimentally demonstrated where the probe wave travels superluminally [20]. In our papers [21, 22] it is shown how one

could use a three- and four-level Raman gain medium together with a PC cavity to create an all-optical switch for the probe beam. Recently, we have proposed electromagnetically induced gratings based on spatial modulation of the Raman gain in a standing-wave pump field [23, 24], which are called Raman induced gratings (RIG). These gratings are fundamentally different from EIAG schemes where the absorption is spatially modulated. Owing to periodic spatial modulation of the Raman gain, the weak probe wave propagates in the forward (a transmitted wave) and backward (a reflected wave) directions. In [23] it is shown that transmitted and reflected wave can be simultaneously amplified at the certain frequency band and the transmission and reflection spectra can be controlled (from amplification to suppression) by varying the pump field intensity. In [24] we shown that transmission and reflection spectra of the RIG can be controlled with the help of an additional control field by varying its intensity or frequency. In this paper, we extend our previous results [23, 24] to further investigate the probe pulse propagation in such a grating. We show that it is possible to control both the amplitude of the probe pulse (with amplification or suppression) and the group velocity from subluminal to superluminal by varying the pump or control field. This structure can operate as an all-optical switch and a transistor.

## II. BASIC THEORY

A model for coherent control of the Raman induced grating is shown schematically in Fig. 1. It can be described by a four-level N-type configuration initially prepared in the ground state  $|0\rangle$ . The ground  $|0\rangle$  and metastable  $|2\rangle$  levels are coupled to the excited level  $|1\rangle$  by a strong pump field at frequency  $\omega_1$  and a weak probe (signal) field at the frequency  $\omega_2$  and wave number  $k_2$ . A strong control field at frequency  $\omega_3$  and wave number  $k_3$  is applied to the transition  $|2\rangle - |3\rangle$

\* Corresponding author: avg@iph.krasn.ru

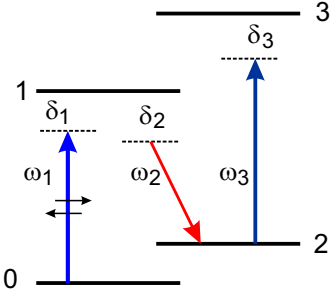


FIG. 1. A schematic diagram of the four-level N-type atomic system for coherent manipulation of the probe (signal) light pulse. The pump field with frequency  $\omega_1$  is a standing wave. The probe pulse has a carrier frequency  $\omega_2$ , and  $\omega_3$  correspond to the control field. The frequency detuning  $\delta_{1,2,3}$  denote the detunings from one-photon resonances for the pump, probe and control fields, respectively.

to enable manipulation by means of the Raman gain. The probe ( $E_s = 1/2E_2 \exp[-i(\omega_2 t - k_2 z)]$ ) and control ( $E_c = 1/2E_3 \exp[-i(\omega_3 t - k_3 z)]$ ) fields propagate along the  $z$  direction and interact with the transitions  $|1\rangle - |2\rangle$  and  $|2\rangle - |3\rangle$ , respectively. The pump field is a standing wave along the  $z$  direction. It is formed by two monochromatic counter-propagating fields  $E_p = 1/2\{E_{1+} \exp[-i(\omega_1 t - k_1 z)] + E_{1-} \exp[-i(\omega_1 t + k_1 z)]\}$ , where  $E_{1+}$  and  $E_{1-}$  are the amplitudes of the forward (+) and backward (-) pump fields with the respective Rabi frequencies  $G_{1+}$  and  $G_{1-}$ . The pump fields are detuned from state  $|1\rangle$  by large one-photon detuning so that single-photon absorption can be neglected. We assume that the Rabi frequency of the probe is much lower than the Rabi frequencies of the pump and control field, which are considered strong fields. The intensity of the pump radiation field is selected such that the threshold of stimulated Raman scattering is not exceeded being, however, high enough to ensure notable amplification of the probe wave. At the same time, spontaneous Raman gain should be much less than the stimulated one.

The induced macroscopic polarization at the probe frequency  $\omega_2$  will be  $P(\omega_2) = N\rho_{21}d_{12} = \chi(\omega_2)E_2$ , where  $N$  is the atomic number density,  $\chi(\omega_2)$  is the linear Raman susceptibility. We assume that the fields are limited to a value such that the change of population of the ground level  $\rho_0$  due to absorption to other levels under applied fields is small, i.e.  $\rho_0 \approx 1$ . The steady-state density matrix equations of motion for the four-level system under the dipole and rotating wave approximation can be written as

$$\begin{aligned} \Delta_2 \rho_{21} &= iG_{1+}^* \rho_{20} - iG_{3+}^* \rho_{31} \\ \Delta_{20} \rho_{20} &= -iG_{2+}^* \rho_{10} + i\rho_{21} G_{1+} - iG_{3+}^* \rho_{30} \\ \Delta_1 \rho_{10} &= -iG_p \rho_0 \\ \Delta_{30} \rho_{30} &= -iG_{32} \rho_{20} + i\rho_{31} G_p \\ \Delta_{31} \rho_{31} &= -iG_{30} \rho_{21} + i\rho_{30} G_p^* \end{aligned} \quad (1)$$

where  $G_p = G_{1+} \exp(ik_1 z) + G_{1-} \exp(-ik_1 z)$ ,  $G_{1\pm} = E_{1\pm} d_{10}/2\hbar$ ,  $G_2 = E_2 d_{12}/2\hbar$ ,  $G_3 = E_3 d_{32}/2\hbar$  denote the

Rabi frequencies of the pump, probe and control fields, respectively,  $\Delta_1 = \gamma_{10} - i\delta_1$ ,  $\Delta_2 = \gamma_{12} - i\delta_2$ ,  $\Delta_3 = \gamma_{32} - i\delta_3$ ,  $\Delta_{30} = \gamma_{30} - i\delta_{30}$ ,  $\Delta_{31} = \gamma_{31} - i\delta_{31}$ , and  $\delta_{1,2,3} = \omega_{1,2,3} - \omega_{10,12,32}$  is the one-photon detuning,  $\delta_{20} = \delta_1 - \delta_2$  is the Raman detuning,  $\delta_{30} = \delta_1 - \delta_2 + \delta_3$ ,  $\delta_{31} = \delta_3 - \delta_2$ ;  $\omega_{mn}$ ,  $\gamma_{mn}$  and  $d_{mn}$  are the frequency, half-width and matrix dipole moment of the respective transitions;  $\hbar$  is the reduced Planck constant. Eqs. (1) are valid if  $|G_2| \ll |G_{1\pm}|$ ,  $|G_3|$ ,  $\delta_1 \gg \gamma_{10}$ ,  $|G_{1\pm}|$ .

The solution for the element  $\rho_{21}$  (to the first order in the probe field and to all orders in the pump and control fields) is

$$\rho_{21} = -i \frac{G_2}{\Delta_1} |G_p|^2 (\Delta_{30} \Delta_{31} + |G_p|^2 - |G_3|^2) / D, \quad (2)$$

where

$$\begin{aligned} D &= (|G_p|^2 - |G_3|^2)^2 + (\Delta_{20} |G_p|^2 + \Delta_{31} |G_3|^2) \Delta_2^* + \\ &\quad (\Delta_{31} |G_p|^2 + \Delta_{20} |G_3|^2) \Delta_{30} + \Delta_{30} \Delta_{20} \Delta_{31} \Delta_2^* \end{aligned}$$

From (2), the susceptibility  $\chi(\omega_2)$  experienced by the probe field can be written as

$$\chi(\omega_2) = -i \frac{\alpha_r \gamma_{10}}{\Delta_1} |G_p|^2 (\Delta_{30} \Delta_{31} + |G_p|^2 - |G_3|^2) / D, \quad (3)$$

where  $\alpha_r = |d_{12}|^2 N / 2\hbar \gamma_{10}$ . When the control field is switched off ( $G_3 = 0$ ), formula (3) is essentially simplified (see the appendix).

Further, we shall assume that the amplitudes of the pump field are real and  $E_{1+} = E_{1-} = E_1$ . In this case, the pump field is a perfect standing wave with the Rabi frequency  $G_p(z) = G_1 \cos(k_1 z)$ , where  $G_1 = E_1 d_{10}/\hbar$ . Susceptibility (3), which depends on  $z$  through  $|G_p(z)|^2 = G_1^2 \cos^2(k_1 z) = G_1^2 [1 + \cos(2k_1 z)]/2$ , is an even periodical function. Thus, susceptibility for the probe field is modulated periodically in space with the period  $\Lambda = \lambda_1/2$ , where  $\lambda_1$  is the wavelength of the pump field. This leads to spatial modulation of the Raman gain and the refractive index. Amplification takes place in the antinodes region of the standing wave, but there is no gain in the nodes. We called such a structure a Raman induced grating [23]. It should be emphasized that this grating is a hybrid one: an amplitude (gain) grating and a phase (refraction) one. Therefore, the probe field propagates in such a medium as in a one-dimensional (1D) periodic structure, i.e. it may propagate both in the forward (the transmitted wave), and backward (reflected wave) direction.

The wave equation for the probe field  $E_2(z)$  in a spatially modulated medium with the susceptibility  $\chi(\omega_2, z)$  in a frequency domain takes the form [25, 26]

$$\frac{d^2 E_2(\omega_2, z)}{dz^2} + k_2^2 [1 + 4\pi\chi(\omega_2, z)] E_2 = 0, \quad (4)$$

where  $k_2 = \omega_2/c$  is the vacuum probe wave number. The solution of (4) can be represented as a superposition of

two waves propagating in opposite directions:

$$E_2(z) = A(z)e^{ik_2z} + B(z)e^{-ik_2z}, \quad (5)$$

where  $A(z)$  and  $B(z)$  are the amplitudes of the forward and backward probe wave, respectively. Using the cosine Fourier expansion  $\chi(\omega_2, z) = \chi_0 + 2 \sum_{n=1}^{\infty} \chi_n \cos(2nk_1z)$  ( $\chi$  is an even function) and the coupled mode analysis [26], we can find the amplitudes  $A(z)$  and  $B(z)$  [23]

$$A(z) = A_0 \frac{s \cos s(L-z) + i(\Delta k - \alpha) \sin s(L-z)}{s \cos(sL) + i(\Delta k - \alpha) \sin(sL)} \quad (6)$$

$$B(z) = A_0 \frac{\sigma \sin s(L-z)}{s \cos(sL) + i(\Delta k - \alpha) \sin(sL)} \quad (7)$$

where  $s = \sqrt{(\Delta k - \alpha)^2 - \sigma^2}$ ,  $\alpha = 2\pi k_2 \chi_0$ ,  $\sigma = 2\pi k_2 \chi_1$ ,  $\Delta k = k_1 - k_2$ .

$$\chi_m(\omega_2) = (k_1/\pi) \int_0^{\pi/k_1} \chi(\omega_2, z) \cos(2mk_1z) dz \quad (8)$$

In defining (6) and (7), we used  $\chi_0$  ( $m = 0$ ) and  $\chi_1$  ( $m = 1$ ), i.e. we restricted ourselves to two spatial harmonics and also used the boundary conditions  $A(z = 0) = A_0$ ,  $B(L) = 0$ , where  $A_0$  is the incident probe wave amplitude (no Fresnel reflection from the interface).

Let us introduce the amplitude coefficients of transmission (gain)  $t(\omega_2, z = L) = A(\omega_2, L)/A_0$  and reflection  $r(\omega_2, z = 0) = B(\omega_2, 0)/A_0$

$$t(\omega_2) = \frac{s \cos(sL)}{s \cos(sL) + i(\Delta k - \alpha) \sin(sL)}, \quad (9)$$

$$r(\omega_2) = \frac{\sigma \sin(sL)}{s \cos(sL) + i(\Delta k - \alpha) \sin(sL)}. \quad (10)$$

Then we can easily obtain the energy transmittance  $T = |t(\omega_2)|^2$  and reflectance  $R = |r(\omega_2)|^2$ .

### III. RESULTS AND DISCUSSION

For numerical simulations we use the parameters corresponding to the  $D1$  line of Na atoms, and the levels  $|0\rangle$  and  $|2\rangle$  are long-lived hyperfine sublevels of the electronic ground state  $3S_{1/2}$ . The atomic parameters are  $\gamma_{10} = 2\pi \times 10$  MHz,  $\gamma_{20} = \gamma_{10}/100$ ,  $N = 10^{12}$  cm $^{-3}$ , and the sample length is  $L = 5$  mm. The Rabi frequency of the pump ( $G_1$ ) and control ( $G_3$ ) fields will be expressed in the units of  $\gamma_{10}$  and the Raman detuning  $\delta_{20}$  in  $\gamma_{20}$  units.

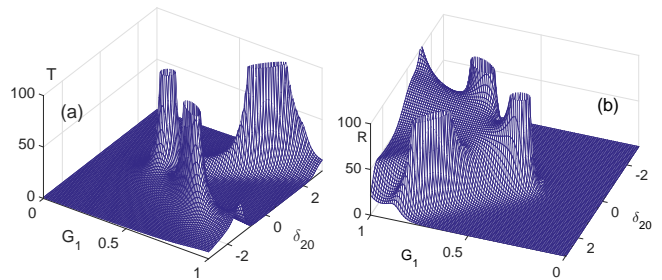


FIG. 2. The transmission (a) and reflection (b) vs Raman detuning  $\delta_{20}$  (in  $\gamma_{20}$  units) and pump Rabi frequency  $G_1$  (in  $\gamma_{10}$  units) in the case when the control field is off ( $G_3 = 0$ ).

#### A. The transmission and reflection spectra

Let us first consider the case when the control field is switched off ( $G_3 = 0$ ). In Fig. 2 the transmission  $T$  and reflection  $R$  for the probe field are plotted as functions of the Raman detuning  $\delta_{20}$  and pump Rabi frequency  $G_1$  at a fixed one-photon detuning  $\delta_1 = -100\gamma_{10}$ . It can be seen that the transmission and reflection spectra strongly depend on the pump field intensity. The transmitted and reflected light can be amplified in some frequency range. Therefore, transmittance and reflectivity can be interpreted as a transmission and reflection gain, respectively. The transmission spectra depend on the Raman detuning  $\delta_{20}$  and have a resonance character at the pump Rabi frequency. As the pump field intensity increases, there occurs a dip in the transmission spectrum near the Raman resonance. The depth and width of the dip increase with the pump intensity and the dip center is shifted due to the Stark shift of the resonance frequency of the Raman transition (see (A1) in Appendix). In the area between the peaks the sample may become opaque ( $T \rightarrow 0$ ). A similar behavior also holds for reflection, but the dip is less pronounced. Away from the Raman resonance, the gain disappears ( $T \rightarrow 1$  and  $R \rightarrow 0$ ). Thus, by changing the intensity of the pump field we can control the transmission (reflection) spectrum of the probe radiation under Raman interaction with a standing wave pump.

The presence of an additional control field ( $\omega_3$  in Fig. 1) leads to essential modification of the propagation properties of the medium [24]. The typical transmission spectrum is shown in Fig.3 as a function of the Raman detuning  $\delta_{20}$  and the control field Rabi frequency  $G_3$ . It is seen that the transmission has a resonant character as a function of  $G_3$ , i.e. peak occurs at the certain values  $G_3$ , and its position depends on the intensity of the pump field. The intensity of the control field decreases with increasing thickness of the sample  $L$ . Note that small variations of the control field intensity can change the system from opaque to transparent (with amplification) and vice versa. In [24] it is shown that in the case of non-perfect standing pump wave with the unequal amplitudes for forward and backward fields, the transmission

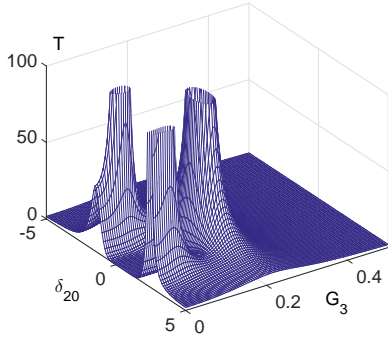


FIG. 3. The transmission spectrum vs Raman detuning  $\delta_{20}$  and control Rabi frequency  $G_3$  (in  $\gamma_{10}$  units) for the case when the pump Rabi frequency  $G_1 = 0.8$ , and the frequency detuning of the control field  $\delta_3 = 0$ .

and reflection spectra qualitatively have the same behavior. And although they are sensitive to the difference between the amplitudes of contradirected pump waves, however it is not critical and does not lead to noticeable changes in the discussed dependencies. A similar behavior occurs for the reflection spectrum.

### B. Control of light-pulse propagation

Using Eqs. (9)–(10) and the Fourier transform method one can study the propagation dynamics of an incident probe pulse assuming that the pump standing wave and the control field are continuous and monochromatic waves. Here, we assume that the input probe pulse has the following Gaussian profile in the time and frequency domains

$$E_{2i}(t) = E_0 \exp(-t^2/\tau^2)$$

$$E_{2i}(\omega_2) = 2^{-1/2}\tau E_0 \exp[-\tau^2(\omega_2 - \omega_{2c})^2/4],$$

where  $E_0$  is the pulse amplitude,  $2\tau = T_{2p}$  is the pulse width at the level  $e^{-1}$ ,  $\omega_{2c}$  is the carrier frequency of the probe pulse. The transmitted and reflected Fourier components can be derived from  $E_{2T}(\omega_2) = t(\omega_2)E_{2i}(\omega_2)$  and  $E_{2R}(\omega_2) = r(\omega_2)E_{2i}(\omega_2)$ . The transmitted and reflected probe pulse in the time domain via inverse Fourier transform is given by

$$E_{2T,2R}(t) = \int_{-\infty}^{\infty} E_{2T,2R}(\omega_2) \exp(-i\omega_2 t) d\omega_2 \quad (11)$$

Let us first consider the case  $G_3 = 0$ , i.e. the control field is off. Fig. 4 shows a typical behavior of the transmitted ( $z = L$ ) and reflected ( $z = 0$ ) probe pulse for different values of the pump Rabi frequency  $G_1$  under Raman resonance for the carrier frequency of the pulse ( $\delta_{2c} = \omega_1 - \omega_{2c} - \omega_{20} = 0$ ). One can see that the transmitted and reflected pulses are sensitive to  $G_1$ . When the Rabi frequency  $G_1$  corresponds to the left branch of

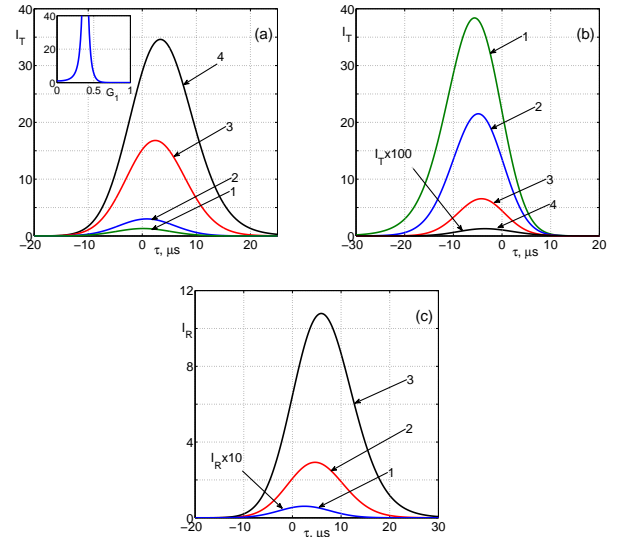


FIG. 4. The transmitted  $I_T$  (a, b) and reflected  $I_R$  (c) probe light pulse for different values of the Rabi frequency  $G_1$  in the case when  $G_3 = 0$ ,  $\delta_{2c} = 0$ . a) 1 -  $G_1 = 0.1$ , 2 -  $G_1 = 0.2$ , 3 -  $G_1 = 0.31$ , 4 -  $G_1 = 0.34$ ; b) 1 -  $G_1 = 0.43$ , 2 -  $G_1 = 0.45$ , 3 -  $G_1 = 0.5$ , 4 -  $G_1 = 0.8$ ; c) 1 -  $G_1 = 0.2$ , 2 -  $G_1 = 0.31$ , 3 -  $G_1 = 0.34$ . The maximum of the reference pulse (not shown) corresponds to  $\tau = 0$ . The inset shows transmission  $T$  as a function of the pump field Rabi frequency.

the curve  $T(G_1)$  (inset in Fig. 4a), the transmitted pulse is amplified and enhances with increasing  $G_1$  (Fig. 4a). In the case when  $G_1$  corresponds to the right branch of the curve  $T(G_1)$ , the pulse amplification decreases with increasing  $G_1$  (Fig. 4b). A similar behavior also takes place for the reflected pulses (Fig. 4c). Thus, the RIG can operate as an all-optical switch and an amplifier. A similar pattern is observed for other detunings  $\delta_{2c}$ .

We also note that the transmitted (reflected) pulse may either lag (Fig. 4a and 4c) or lead (Fig. 4b) the reference pulse (not shown), which covers the same distance in a vacuum. Therefore, we can speak about subluminal propagation of the probe pulse, when the pulse group velocity is less than the speed of light in vacuum (a slow light), or superluminal propagation, when the group velocity is negative or higher than the speed of light in vacuum (fast light) [27].

Group delay for the transmitted and reflected pulse can be calculated as [28]

$$\tau_g^{T,R} = \left( \frac{\partial \Phi_{T,R}}{\partial \omega_2} \right)_{\omega_2 = \omega_{2c}}$$

where  $\Phi_{T,R}$  are the phase of the transmission  $t(\omega_2)$  and reflection  $r(\omega_2)$  coefficient, respectively. A positive group delay (the pulse at the output appears later than the reference) corresponds to the subluminal propagation. A negative group delay (the pulse at the output appears earlier than the reference) corresponds to the superluminal propagation. The inset in Fig. 5 shows the group de-

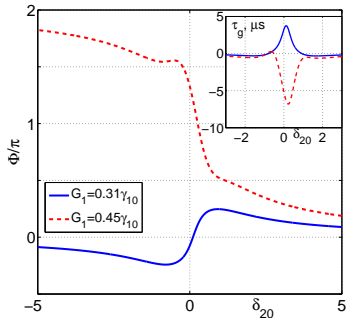


FIG. 5. Spectral dependences of the phase of the transmitted probe wave for the Rabi frequencies  $G_1 = 0.31$  and  $G_1 = 0.45$ . Inset: the group delay  $\tau_g$  as a function of detuning from the Raman resonance  $\delta_{2c}$  for the same  $G_1$ .

lay  $\tau_g$  as a function of the detuning  $\delta_{20}$  for the values  $G_1$  corresponding to the curves 3 (Fig. 4a) and 2 (Fig. 4b). In the first case ( $G_1 = 0.31$ )  $\tau_g > 0$  (subluminal propagation) and in the second case ( $G_1 = 0.45$ )  $\tau_g < 0$  (superluminal propagation). Calculations show that subluminal propagation occurs when the Rabi frequency  $G_1$  corresponds to the left branch of the dependence  $T(G_1)$  (see the inset in Fig. 4a), where normal dispersion for the probe wave is realized (Fig. 5). When  $G_1$  corresponds to the right branch of the dependence  $T(G_1)$ , superluminal propagation arises since dispersion for the probe wave becomes anomalous (Fig. 5). The mechanism of attaining normal and anomalous dispersion is associated with dispersion of the RIG (structural dispersion) rather than the Raman medium (material dispersion).

The presence of a control field opens new possibilities for manipulating the propagation dynamics of the probe pulse. Fig. 6 illustrates the transmitted and reflected Gaussian probe pulse for various Rabi frequencies  $G_3$  at different values of the pump Rabi frequency  $G_1$  (the operating point). The pulse propagation dynamics depends essentially on the Rabi frequency  $G_3$ . Figs. 6a, b show the transmitted and reflected probe pulse in the case when the Rabi frequency  $G_1$  corresponds to the left branch of the curve  $T(G_1)$  or  $R(G_1)$ , respectively. Selecting the intensity of the control field, we can suppress the reflected pulse. In this case, RIG acts as a controllable amplifier for transmitted and reflected pulses. Note that here we deal with subluminal pulses ( $\tau_g > 0$ ) and  $\tau_g$  depends on  $G_3$ .

Fig. 6c shows the case when the intensity of the pump field is selected such that transmittance of the grating is close to zero (at  $G_3 = 0$ ). When the control field is turned on the pulse amplification increases with  $G_3$  (curves 2 and 3 in Fig. 6a) as long as the Rabi frequency  $G_3$  corresponds to the left branch of the curve  $T(G_3)$  (the inset in Fig. 6a). When  $G_3$  corresponds to the right branch, the pulse amplification decreases with increasing  $G_3$ . Meanwhile, the group velocity of the pulse also changes from subluminal to superluminal. Thus, by changing the con-

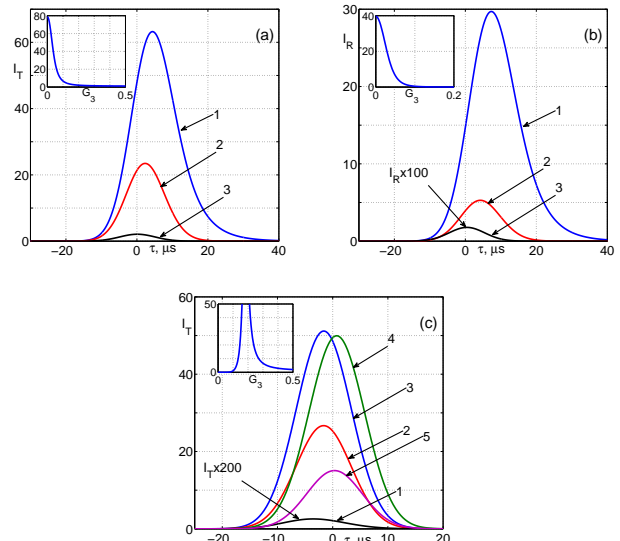


FIG. 6. The transmitted ( $I_T$ ) and reflected ( $I_R$ ) probe light pulse for different values of the Rabi frequency  $G_1$  and  $\delta_{32} = 0$ ,  $\delta_{2c} = 0$ . (a), (b):  $G_1 = 0.36$ , 1 -  $G_3 = 0$ , 2 -  $G_3 = 0.05$ , 3 -  $G_3 = 0.2$ . (c):  $G_1 = 0.8$ , 1 -  $G_3 = 0$ , 2 -  $G_3 = 0.15$ , 3 -  $G_3 = 0.16$ , 4 -  $G_3 = 0.21$ , 5 -  $G_3 = 0.25$ . The insets show the transmission  $T$  (a, c) and reflection  $R$  (b) as a function of the control field Rabi frequency  $G_3$ .

trol field intensity we can change the system from opaque to transparent (with amplification) and vice versa, i.e., this structure can operate as an all-optical transistor.

#### IV. CONCLUSION

We have presented a theoretical study on the probe light pulse propagation under Raman interaction with a pump standing wave in three- and four-level media. For a three-level atomic system, we show that, it is possible to control both the transmission (reflection) of the probe pulse and the dispersion of RIG (structural dispersion) by changing the intensity of the pump field. Herewith the dispersion can be changed from normal to abnormal, and we can therefore manipulate the pulse group velocity from subluminal to superluminal. We have also shown that adding a control field coupled to a fourth state, the properties of the weak probe light pulse propagation are greatly changed. In particular small variations in the intensity of control field transfer the system from the opaque to transparent (with amplification) state and vice versa. Therefore this structure can operate as an all-optical transistor. At the same time, it can be used as a nonlinear controllable mirror with the reflectivity greater than unity. Also due to the variation of the control field intensity, the probe pulse propagation can be changed from subluminal to superluminal. This opens new possibilities to manipulate the dispersion and transmission and may be used in different fields of applied photonics.

The intensity of the control and pump field strongly depends on a number of parameters (detuning from one-photon and Raman resonances, a Raman resonance width, a sample thickness and others). The required laser fields intensity is tens–hundreds mW/cm<sup>2</sup> for the pump field and 2-3 orders of magnitude lower for the control field.

### ACKNOWLEDGMENTS

This work was supported by the Russian Foundation for Basic Research under Grant No. 15-02-03959.

### Appendix A:

In the appendix, we give the formula for the susceptibility  $\chi(\omega_2, z)$  for the case when the control field is off ( $G_3 = 0$ ) and calculate the Fourier components (8)  $\chi_0$  and  $\chi_1$  in this case. It is not difficult to show that when  $G_3 = 0$  and  $|\delta_1| \gg \gamma_{10}$ ,  $|\delta_2| \gg \gamma_{12}$  susceptibility (3) simplifies to

$$\chi(\omega_2, z) = \frac{\alpha_r \gamma_{10}}{\delta_1} \frac{G_1^2 [1 + \cos(2k_1 z)] / 2}{\delta_2 [\delta_{20} + G_1^2 / 2\delta_2 + i\gamma_{20} + G_1^2 \cos(2k_1 z) / 2\delta_2]} \quad (\text{A1})$$

From Eq. (A1) we see that a strong pump field ( $G_1^2 / |\delta_2| \gg \gamma_{20}$ ) causes a shift in the resonance frequency of the Raman transition (the Stark shift). In the case of a weak pump field ( $G_1^2 / |\delta_2| \ll \gamma_{20}$ ) Eq. (A1) is consistent with the standard Raman susceptibility as defined in the perturbation theory [16].

For susceptibility (A1) the spatial Fourier components  $\chi_0$  and  $\chi_1$  are calculated analytically. To calculate integrals (8) for the  $\chi(\omega_2, z)$ , formula (A1) is conveniently

rewritten as

$$\chi(\omega_2, z) = \frac{\alpha_r \gamma_{10}}{\delta_1} \frac{A [1 + \cos(2k_1 z)]}{1 + A \cos(2k_1 z)}, \quad (\text{A2})$$

where  $A = \frac{G_1^2}{2\delta_2} \frac{1}{\delta_{20} + G_1^2 / 2\delta_2 + i\gamma_{20}}$ .

Then

$$\chi_0 = \frac{k_1}{\pi} \frac{\alpha_r \gamma_{10}}{\delta_1} A \int_0^{\pi/k_1} \frac{1 + \cos(2k_1 z)}{1 + A \cos(2k_1 z)} dz = \frac{\alpha_r \gamma_{10}}{\delta_1} \frac{1 - A + \sqrt{1 - A^2}}{1 + A} \quad (\text{A3})$$

$$\chi_1 = \frac{k_1}{\pi} \frac{\alpha_r \gamma_{10}}{\delta_1} A \int_0^{\pi/k_1} \frac{1 + \cos(2k_1 z)}{1 + A \cos(2k_1 z)} \cos(2k_1 z) dz = \frac{\alpha_r \gamma_{10}}{\delta_1} \frac{A^2 - 1 + \sqrt{1 - A^2}}{A(1 + A)} \quad (\text{A4})$$

Numerical simulations using formula (8) with  $G_3 = 0$  are

in good agreement with the analytical results (A3)–(A4).

- 
- [1] M. Notomi, Reports on Progress in Physics **73**, 096501 (2010).  
 [2] N. N. Rozanov, S. V. Fedorov, R. S. Savel'ev, A. A. Sukhorukov, and Y. S. Kivshar, JETP **114**, 782 (2012).  
 [3] D. N. Neshev, A. A. Sukhorukov, A. Mitchell, C. R. Rosenberg, R. Fischer, A. Dreischuh, W. Z. Krolikowski, and Y. S. Kivshar, in *14th International School on Quantum Electronics: Laser Physics and Applications*, Proc. SPIE, Vol. 6604 (2007) pp. 66041B–66041B–15.  
 [4] M. Fleischhauer, A. Imamoglu, and J. P. Marangos, Rev. Mod. Phys. **77**, 633 (2005).  
 [5] X. M. Su and B. S. Ham, Phys. Rev. A **71**, 013821 (2005).  
 [6] J.-H. Wu, A. Raczynski, J. Zaremba, S. Zienińska-

- Kaniasty, M. Artoni, and G. La Rocca, J. Mod. Optics **56**, 768 (2009).  
 [7] A. André and M. D. Lukin, Phys. Rev. Lett. **89**, 143602 (2002).  
 [8] M. Artoni and G. C. La Rocca, Phys. Rev. Lett. **96**, 073905 (2006).  
 [9] M. Bajcsy, A. S. Zibrov, and M. D. Lukin, Nature **426**, 638 (2003).  
 [10] S. A. Moiseev, A. I. Sidorova, and B. S. Ham, Phys. Rev. A **89**, 043802 (2014).  
 [11] A. W. Brown and M. Xiao, Opt. Lett. **30**, 699 (2005).  
 [12] H. Y. Ling, Y.-Q. Li, and M. Xiao, Phys. Rev. A **57**, 1338 (1998).

- [13] X. M. Su, Z. C. Zhuo, B. S. Ham, and J. B. Kim, J. Korean Phys. Soc. **51**, 48 (2007).
- [14] E. Paspalakis and P. L. Knight, Phys. Rev. A **63**, 065802 (2001).
- [15] C. Liu, S. Gong, D. Cheng, X. Fan, and Z. Xu, Phys. Rev. A **73**, 025801 (2006).
- [16] R. W. Boyd, *Nonlinear optics* (London: Academic Press, 1992).
- [17] K. J. Jiang, L. Deng, and M. G. Payne, Phys. Rev. A **74**, 041803 (2006).
- [18] K. J. Jiang, L. Deng, and M. G. Payne, Phys. Rev. A **76**, 033819 (2007).
- [19] K. J. Jiang, L. Deng, E. W. Hagley, and M. G. Payne, Phys. Rev. A **77**, 045804 (2008).
- [20] R. B. Li, L. Deng, and E. W. Hagley, Phys. Rev. Lett. **110**, 113902 (2013).
- [21] V. G. Arkhipkin and S. A. Myslivets, Phys. Rev. A **80**, 061802 (2009).
- [22] V. G. Arkhipkin and S. A. Myslivets, Phys. Rev. A **88**, 033847 (2013).
- [23] V. G. Arkhipkin and S. A. Myslivets, Opt. Lett. **39**, 3223 (2014).
- [24] V. G. Arkhipkin and S. A. Myslivets, Phys. Rev. A **93**, 013810 (2016).
- [25] S. Rautian, Opt. Spectrosc. **104**, 112 (2008).
- [26] S. Y. Karpov and S. N. Stolyarov, Physics-Uspekhi **36**, 1 (1993).
- [27] P. W. Milonni, *Fast Light, Slow Light and Left-Handed Light* (Taylor & Francis Group, New York, 2005).
- [28] V. S. C. Manga Rao, S. Dutta Gupta, and G. S. Agarwal, Opt. Lett. **29**, 307 (2004).